Nature Environment and Pollution Technology
An International Quarterly Scientific Journal

p-ISSN: 0972-6268
(Print copies up to 2016)
e-ISSN: 2395-3454

Vol. 21 | No. 5 (Suppl) | pp. 2315-2321 | 2022

Original Research Paper

https://doi.org/10.46488/NEPT.2022.v21i05.027

Open Access Journal

Satellite-Based Statistical Analysis of Hilla River Water Quality Parameters, Iraq

Fatimah D. Al-Jassani*, Hussein A. M. Al-Zubaidi† and Nisren J. Al-Mansori*****

Department of Environmental Engineering, College of Engineering, University of Babylon, Babylon, Iraq

†Corresponding author: Hussein A. M. Al-Zubaidi; alzubaidih10@gmail.com

Nat. Env. & Poll. Tech.
Website: www.neptjournal.com

Received: 17-06-2022
Revised: 21-07-2022
Accepted: 30-07-2022

Key Words:
Linear regression
Statistical analysis
Water quality modeling
Hilla river

ABSTRACT

Since industrial and human activities have been developed, water quality intensely degrades in Hilla River, Iraq. Using remote sensing technology provides data for assessing and monitoring water quality in surface water bodies. Thus, in this study, Landsat 8 satellite images (2016 to 2021) were statistically tested for developing linear models capable of estimating water quality parameters in the river based on field data, including turbidity (turb), electric conductivity (EC), hydrogen ions (pH), total suspended solids (TSS), chloride ions (Cl), sulfate ions (SO_4), Alkalinity (ALK), total hardness (TH), calcium (Ca), potassium (K), sodium (Na), magnesium (Mg), and total dissolved solids (TDS). The results showed that seven parameters have a significant relationship with the spectral bands ratio (p-value less than 0.05). Some of them (TDS, SO_4, and ALK) are positively correlated with bands ratio (Band10/Band3, Band10/Band3 and Band10/Band4, and Band3/Band7), respectively. Others (Mg, Ca, TH and pH) are inversely correlated with (Band4/Band7, Band1/Band4, Band1/Band4, and Band1/Band2), respectively. However, K, Na, TDS, Cl, EC and turb have an insignificant correlation with any band ratio.

INTRODUCTION

Surface water bodies are used for many purposes involving drinking water sources, recreation, transportation, and aesthetics. With several uses, these water forms are subjected to natural and human activities that can impact water quality. As a result, mechanisms to help protection of surface water, maintain present water quality, or prevent surface water deterioration seem to be critical. Water quality can be assessed according to its chemical, physical, and biological characteristics (Al-Zubaidi 2012, Issa et al. 2013). Water quality indicators, involving biological, chemical, and physical characteristics, have been usually measured by taking samples in the field and then studying them in the laboratory. Though in-situ measurement offers excellent accuracy, it is a labor-intensive and time-consuming operation, making a simultaneous water quality database on a regional scale geographically and temporally impractical (Goetz et al. 2008, Kibena et al. 2014). Remote sensing (RS) methods have become helpful instruments to attain this objective due to the improvements in space science, greater usage of computer applications, and improved computational power in recent periods. Remote sensing methods provide more effective and effectual observing and identification of large-scale areas and water bodies that suffer from qualitative issues (Al-Masaodi & Al-Zubaidi 2021, Alparslan et al. 2007, El-Amier et al. 2017, Hadjimitsis et al. 2010, Markogianni et al. 2018).

To explore the relationships between water quality indicators and spectral data from satellite images, decision-makers in water resources may utilize remote sensing data to better monitor water bodies (Chabuk 2022). Gholizadeh et al. (2016) summarized the characteristics of the main sensor (temporal, spatial, and spectral) utilized for water quality monitoring. This study also examines the methodologies and sensors utilized to assess and quantify the water quality parameters such as COD, BOD, dissolved oxygen, sea surface salinity, total phosphorus, water temperature, turbidity, TSS, Secchi disk depth, colored dissolved organic matter, and chlorophyll-a (chl-a). Japitana & Burce (2019) gave a global perspective of the earth's surface that may be utilized to monitor and analyze water quality using Landsat 8 and regression analysis to predict pH, dissolved oxygen, TDS, TSS, and BOD. The input images were radiometrically calibrated utilizing FLAASH and then atmospherically adjusted to create surface reflectance (SR) bands for comparison. Input data included SR bands produced by FLAASH and DOS algorithm, water indices, band ratios, and PCA images. The input bands' feature vectors were then regressed utilizing the water quality data.

All water quality metrics exhibited relatively high R-squared magnitudes except TSS and conductivity which had 60.1 and 67.7%, respectively. In addition, pH, BOD, TSS, and conductivity regression models are extremely significant to SR bands calculated utilizing DOS. The findings also revealed the possibility of employing RS-based water quality models for periodic water quality monitoring and evaluation. Al-Bayati et al. (2018) investigated field Spector-radiometers by developing relationships between water quality parameters and spectral data. The study included 20 stations for sampling on Hilla River, Babylon Province, Iraq to measure the physical and chemical parameters (pH, TSS, EC, TDS, CL). Landsat 8 satellite images were employed to be linked with field data statistically for only one day of investigation. It has been found that apposite spectral ranges and bands for water quality parameters, EC, and CL associated with a spectra range of (0.851-0.87) µm and (2.107-2.294) µm, respectively. Also, (TSS and Turb), and TDS at a spectral range of (0.533-0.590) µm and (1.566-1.561) µm, respectively. Abbas et al. (2021) utilized Landsat 8 satellite images to estimate total TDS, EC, NO_3, and pH. These models offer the capability of evaluating the water quality parameters dispersal lengthways of the Shatt Al-Arab River in the south of Iraq. Results built on R-squared, RMSE, SE, and p-value highlighted the feasibility of these models for the study area. The four bands (band 2, band 3, band 4, and band 5) of Landsat 8 were used to develop the water quality models. EC models are estimated for the winter, summer, and autumn seasons based on band 5 for winter and band 4 for the summer and autumn seasons. For NO_3 models, it was linked with band 4, band 3, and band 2 for winter, spring, and summer, respectively. pH models were developed depending on a single band for all seasons (band 4, band 5, band 4, and band 5 for winter, spring, summer, and autumn, respectively). For the remaining parameter (TDS), it was a too complex model in this study. One of them was estimated by combining band 3, band 4, and band 5 in terms of band ratios.

Thus, to cover the region of interest in this paper, statistical linear models and correlation analyses were performed between Landsat 8 images and water quality measurements for Hilla River at Hilla City, Iraq spatially along the river and temporally from 2016 to 2021 based on available data from the Ministry of Water Resources, Iraq.

MATERIALS AND METHODS

Study Area and Datasets

Hilla City is located in the center of Iraq on the Hilla River. The river is a branch of the Euphrates River, 100 km south of Baghdad City. Hilla City is the capital of Babylon Province where the ancient city of Babylon is located. It is located in a mainly agricultural region that is widely irrigated from the river, producing a wide range of crops, fruit, and textiles. Fig. 1 shows the present study area. It is situated between, Longitude (44º26'55" & 44º31'10") E and Latitude (32º26'30" & 32º31'33") N.

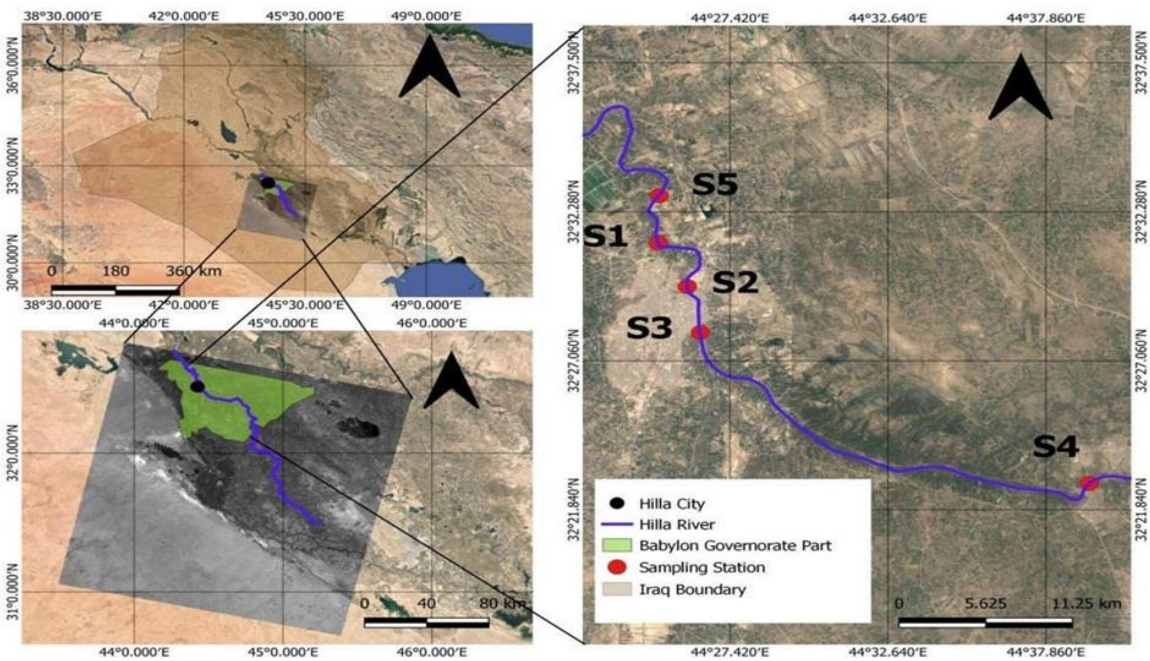

Fig. 1: Map of the study area.

Five stations were selected along the Hilla River. Station 1 (S1): The New Hilla Water Treatment Plant is located in the center of Hilla City in the Zuweir district. It was built in 1991 and produces about 6000 $m^3.h^{-1}$ for Hilla City consumption; Station 2 (S2): The Old Al-Tayarah Water Treatment Plant is located in the Hilla City center of the Al-Tayarah district. It was built in 1972 and produces about 1200 $m^3.h^{-1}$ for the Hilla City consumption too; Station 3 (S3): Al-Hashmiya Water Project with a capacity of 6000 m^3 to serve the districts of Al-Hashmiya, Al-Shuwaili, Al-Qasim and Al-Tali`ah in the Province of Babylon; Station 4 (S4): Al-Atayej Project is located in the city center (in the tourist area), and it produces 900 $m^3.h^{-1}$, and Station 5 (S5): The Annanah Water Project is situated on the right bank of the Hilla River near the village of Annanah. Samples were collected sparsely by Babylon Water Resources Directorate, Iraq at each sampling station from January 2016 to June 2021. The collection process included taking one or two samples monthly during this period. Table 1 displays the yearly averaged water quality parameters magnitudes.

Hilla City is situated between path 168 and row 38 of the Landsat 8 satellite. To discover the relations between water quality indicators and spectral data from the satellite, Landsat 8 senses were downloaded from the United States Geological Survey (USGS) website at the same sampling time and for the entire study period, covering the sampling process spatially and temporally (Fig. 1).

Methodology

The general structure of this study is displayed in Fig. 2 which is the conceptual model of the study. In-site water quality data from the five sampling stations and the related images from the Landsat 8 satellites were linked by linear models statistically. In-situ data was split into two datasets: train and test. The Landsat 8 images were collected 2 level 2 (surface reflectance) that contains 8 spectral bands (1 to 7 and 10) (Hereher et al. 2010, Kontopoulou et al. 2017). The GIS analysis was carried out utilizing QGIS software in order to display the spatial distribution of the spectral bands to be correlated with field data. The boundary of the river was digitized to make the polygon shape of the river extract the river water (El-Zeiny & El-Kafrawy 2017). After extracting the surface reflectance of each band from Landsat senses, RStudio software was utilized to develop linear models

Table 1: *In-situ* water quality parameters employed in this study.

Sampling Station	Year	Water Quality Parameter												
		k	Na	TSS	TDS	SO_4	Cl	Mg	Ca	TH	ALK	EC	pH	Turb
S1	2016	4.0	84.2	62.7	704.0	297.3	111.8	40.2	87.2	381.7	120.0	1086.5	7.8	15.4
	2017	3.0	81.3	25.0	662.0	230.3	107.3	29.8	74.0	314.0	134.0	1015.5	7.8	6.4
	2018	3.2	82.6	32.0	685.2	273.8	123.2	34.8	89.8	362.4	138.4	1135.8	7.2	7.0
	2019	2.9	48.7	44.7	596.0	250.3	75.3	25.0	105.7	366.3	147.3	949.0	7.4	24.2
	2020	3.7	72.0	38.0	630.0	248.0	85.0	33.5	96.5	378.5	108.0	960.0	7.3	10.1
	2021	3.3	72.5	36.0	645.0	280.0	87.0	34.0	93.0	371.5	101.0	1019.0	7.9	6.4
S2	2016	3.2	85.5	44.5	707.0	324.8	106.3	36.8	94.0	385.5	113.5	1105.0	7.9	15.1
	2017	3.0	67.1	29.6	653.2	247.0	109.6	33.2	76.0	330.6	134.8	1052.6	7.8	11.6
	2018	3.4	86.7	44.7	685.3	285.3	120.7	32.0	86.7	347.7	128.7	1139.7	6.9	7.4
	2019	2.8	47.3	32.0	605.3	249.7	74.3	24.0	106.0	362.7	146.0	954.0	7.5	15.5
	2020	3.2	67.5	37.5	606.0	252.8	82.3	34.0	98.3	385.3	123.5	952.8	7.5	12.5
	2021	3.3	71.0	68.7	600.7	254.3	90.0	36.7	80.7	352.0	110.0	996.0	7.6	12.8
S3	2016	6.8	91.0	42.0	758.0	365.0	122.0	41.0	106.0	432.0	112.0	1175.0	8.1	19.0
	2019	3.1	66.0	46.0	630.0	244.0	95.0	32.0	101.0	384.0	140.0	1048.0	7.2	2.9
	2021	3.4	72.0	42.0	554.0	206.0	91.0	35.0	69.0	314.0	110.0	947.0	7.1	7.1
S4	2016	3.3	85.5	70.0	731.0	317.5	110.0	38.5	89.0	380.0	109.0	1132.5	8.0	12.4
	2017	3.0	83.7	61.3	660.7	266.7	109.3	36.3	75.3	341.0	126.7	1036.3	7.7	13.9
	2018	2.9	86.0	14.0	630.0	258.0	116.0	35.0	84.0	352.0	120.0	1072.0	6.7	5.2
	2021	3.7	69.0	30.0	552.0	217.5	89.5	37.0	68.0	321.0	110.0	937.0	7.7	5.6
S5	2016	3.1	84.0	37.0	690.0	314.0	114.5	37.0	91.0	379.5	118.0	1079.0	7.9	8.4
	2017	3.0	79.7	29.3	660.7	242.7	113.7	32.0	79.0	334.7	127.3	1054.7	8.0	3.1
	2018	3.2	87.5	30.0	723.0	259.5	142.0	38.0	87.0	372.0	143.0	1174.0	7.4	7.4
	2020	4.7	76.0	22.0	544.0	212.0	85.0	39.0	78.0	353.0	116.0	912.0	7.5	27.4

between the train water quality parameters and the spectral bands. Finally, the test dataset was utilized to validate the developed model's robustness.

RESULTS AND DISCUSSION

Data Exploration

Many water quality parameters were measured from 2016 to 2021 including turbidity magnitude (Turb), (EC), (pH), (TSS), (Cl), (SO_4), (ALK), (TH), (Ca), (TDS), (Mg), (Na), and (K). A graphical summary (boxplots) of the water quality parameters is shown in Figs. 3 and 4. Raw data statistically reveals outliers' existence, however, these outliers will be kept because they could be related to errors or mistakes during sample gatherings such as errors due to parameter measurements, calculations, or any other source that could change the measured magnitudes (Al-Zubaidi et al. 2021). Fig. 5 highlights the correlation between water quality parameters. The best relation between parameters has a correlation coefficient close to 1 and a p-value less than 0.05 such as TDS with EC, TDS with SO4, SO4 with TH, and CL with EC. Many parameters have a normal distribution in the river. This can be visually noticed in the correlation plot, see the histogram plots of the parameters in Fig. 5. The Shapiro–Wilk test was utilized to confirm the normality quantitatively, see Table 2. The test showed that the w-value was close to 1 and the p-value greater than 0.05 for many parameters, except for TSS, K, Na, SO_4, and Turb.

Linear Models Development and Statistical Analysis

The linear regression model for the water quality parameters and the band ratio values of the satellite data are shown in Table 3. Statistical results for the 13 water quality parameters showed that 7 parameters have a significant relation with band ratio (p-value less than 0.05). These parameters were lineally regressed with the related band ratio by a linear model. The resulting models of the 7 parameters with bands ratio have a p-value less than 0.05. TDS is positively correlated with B10/B3 ($P = 0.034$), SO4 is positively correlated with B10/B3 and B10/B4 ($P = 0.001$), Mg is inversely correlated with B4/B7 ($P = 0.003$), Ca is inversely correlated with B1/B4 ($P = 0.038$), TH is inversely correlated with B1/B4 ($P = 0.024$), ALK is positively correlated with B3/B7 ($P = 0.016$), and pH is inversely correlated with B1/B2 ($P = 0.003$). The remaining parameters (K, Na, TDS, Cl, EC, and Turb) have an insignificant correlation with the bands ratio (p-value greater than 0.05). The MAE and RMAE show the difference between the measured data and the

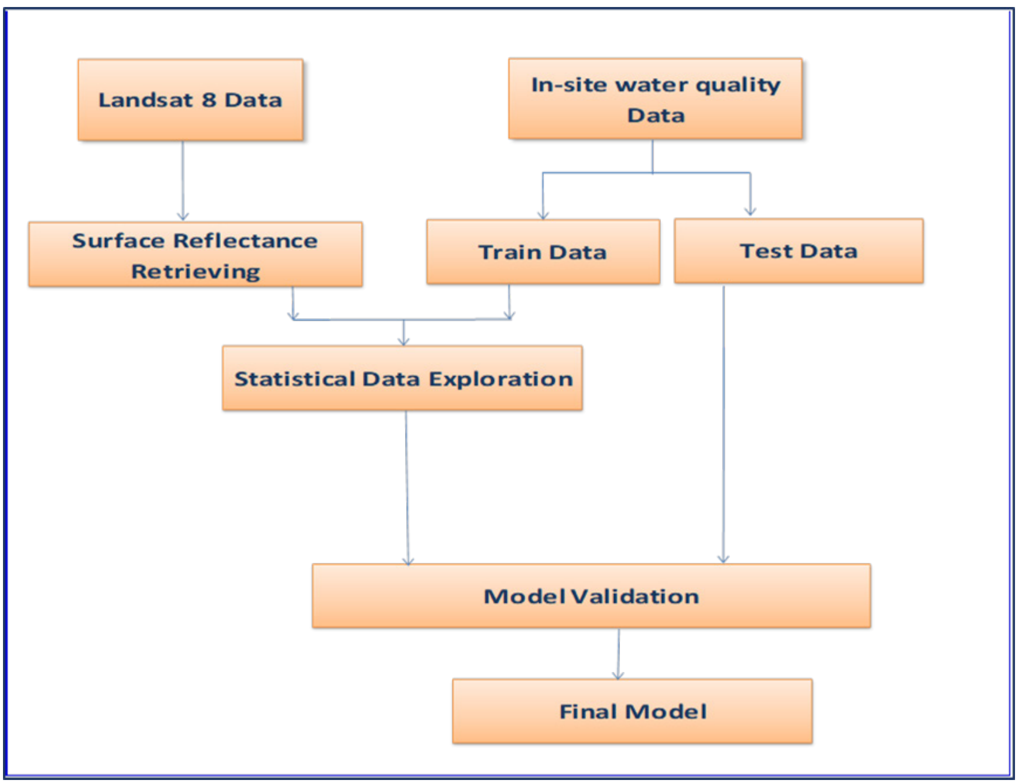

Fig. 2: Data processing flowchart.

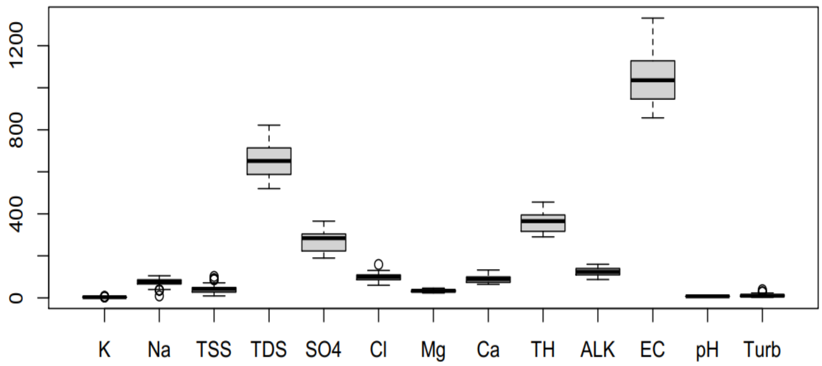

Fig. 3: Boxplots of all water quality parameters used in the study.

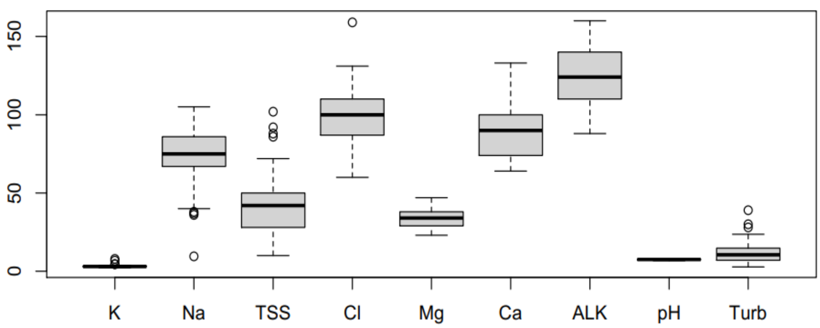

Fig. 4: Boxplots of the water quality parameters used in the study after excluding EC, TH, SO_4, and TDS.

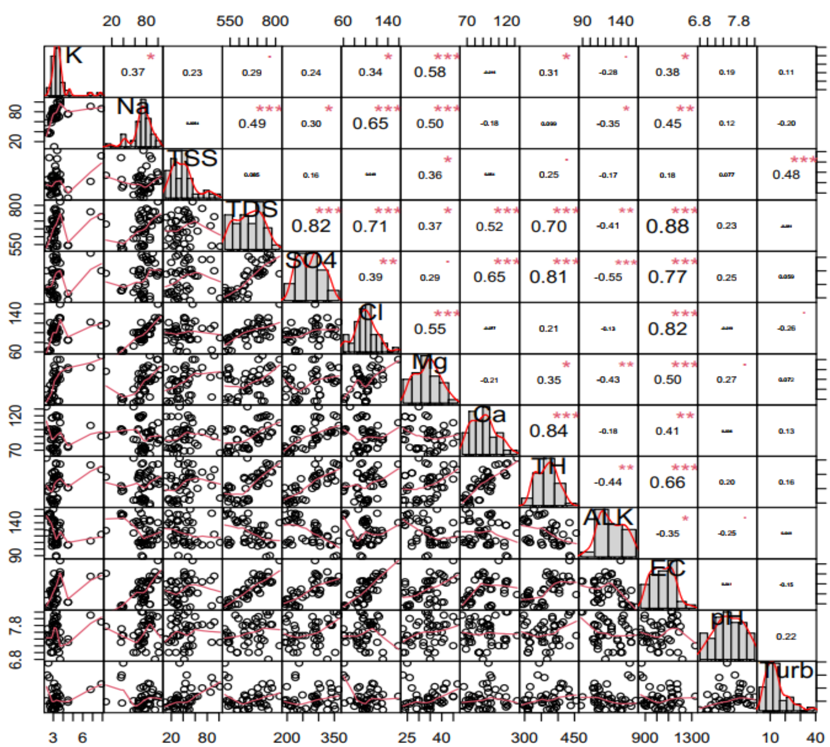

Fig. 5: Correlation plot of water quality parameters.

Table 2: Shapiro-Wilk test for water quality parameter.

Water quality parameter	w-value	p-value	Normality case
pH	0.9736	0.3879	Normal
TDS	0.9562	0.0873	Normal
TSS	0.9221	0.005	Not normal
K	0.62398	1.68E-09	Not normal
Na	0.9126	0.0024	Not normal
SO_4	0.9337	0.0127	Not normal
Cl	0.9742	0.4078	Normal
Mg	0.96445	0.1803	Normal
Ca	0.9555	0.0825	Normal
TH	0.95907	0.1125	Normal
ALK	0.95459	0.07588	Normal
EC	0.9624	0.1513	Normal
Turb	0.88487	0.000331	Not normal

model predictions. The best result was for pH with very low errors.

CONCLUSION

Remote sensing and GIS techniques in combination with in-situ measurements are the most effective, cheaper, and more dependable tools for observing water quality parameters in several surface water bodies (rivers, lakes, and reservoirs). The main findings of this study showed a significant correlation between in-situ measurements and remote sensed-based datasets in Hilla River, Iraq. The developed linear models can be utilized in estimating water quality parameter parameters (TDS, SO_4, Mg, Ca, TH, ALK, and pH) and predicting their seasonal changes. To apply the developed models for future predictions, it is not essential to obtain high-resolution and commercial satellite images since a free satellite image such as the Landsat series can be a dependable input image if the accurate pre-processing method is employed. In addition, MAE and RMAE are effective scales to validate the regressed model since they depict the difference between the model predictions and real data in the same unit of measurement.

ACKNOWLEDGMENT

The authors thank the Department of Environmental Engineering, at the University of Babylon for their support in doing this research.

REFERENCES

Abbas, M.R., Ahmad, B.B. and Abbas, T.R. 2021. Statistical remote sensing for prediction of inland water quality parameters for Shatt Al-Arab River in Iraq. IOP Conf. Ser. Earth Environ. Sci., 16: 111

Al-Bayati, Z.M.K., Nayle, I.H. and Jasim, B.S. 2018. Study of the relationship between spectral reflectivity and water quality index in Hilla River. Int. J. Eng. Technol., 7(3): 196-200.

Al-Zubaidi, H.A.M., Naje, A.S., Abed Al-Ridah, Z., Chabuck, A. and Ali, I M. 2021. A statistical technique for modeling dissolved oxygen in salt lakes. Cogent Eng., 8(1): 1875533.

Al-Zubaidi, H.A.M. 2012. Effect of heavy metals in wastewater effluents of Textile Factory-Hilla on the characteristics of Hilla River. J. Kerbala Univ. Sci., 10(3): 5-16.

Al-Masaodi, H.G.O. and Al-Zubaidi, H.A.M 2021. Spatial-temporal changes of land surface temperature and land cover Babylon Governorate, Iraq. Mater. Today Proceed., 5: 179. https://doi.org/10.1016/j.matpr.2021.05.179.

Alparslan, E., Aydöner, C., Tufekci, V. and Tüfekci, H. 2007. Water quality

Table 3: Remote sensing-based regression models for the selected water quality parameter parameters.

Water quality parameter	cor.	p-value	Bands ratio	Model	MAE	RMAE
pH	-0.43	0.00352	B1/B2	pH = 13.886 - 6.841*B1/B2	0.35	0.46
TDS	0.32	0.034	B10/B3	TDS = 276 + 86.16*B10/B3	76.1	89.7
TSS	-0.03	0.37276	B1/B2	-	-	-
K	0.24	0.10946	B6/B1	-	-	-
Na	-0.28	0.06742	B4/B7	-	-	-
SO_4	0.39	0.001604	B10/B3 +B10/B4	SO_4= 156.99 + 134.19*B10/B3 - 99.2*B10/B4	44.9	47.0
Cl	0.21	0.08636	B1/B2	-	-	-
Mg	-0.42	0.00385	B4/B7	Mg = 65.215 - 28.599*B4/B7	4.6	6.1
Ca	-0.31	0.0382	B1/B4	Ca = 158.18 - 77* B1/B4	11.4	13.5
TH	-0.33	0.02451	B1/B4	TH = 547.91 - 210.5* B1/B4	36.0	40.7
ALK	0.4	0.01675	B3/B7	ALK = 55.95 + 57.95* B3/B7	12.4	14.5
EC	0.08	0.58264	B1/B2	-	-	-
Turb	-0.25	0.09302	B7/B10	-	-	-

cor.: Pearson Correlation, MAE: Mean Absolute Error, RMAE: Root Mean Squared Error.

assessment at Ömerli Dam using remote sensing techniques. Environ. Monit. Assess., 135(1): 391-398.

Chabuk, A., Al-Zubaidi H.A.M., Abdalkadhum A.J., Al-Ansari N., Ali Abed S., Al-Maliki A. and Ewaid, S. 2022. Application ArcGIS on the Modified-WQI Method to Evaluate the Water Quality of the Euphrates River, Iraq, Using Physicochemical Parameters. Proceedings of Sixth International Congress on Information and Communication Technology, 25-26 Feb 2022, Brunei University, London, Springer, Singapore, pp. 657-675.

El-Amier, Y.A., Elnaggar, A.A. and El-Alfy, M.A. 2017. Evaluation and mapping spatial distribution of bottom sediment heavy metal contamination in Burullus Lake, Egypt. Egypt. J. Basic Appl. Sci., 4(1): 55-66.

El-Zeiny, A. and El-Kafrawy, S. 2017. Assessment of water pollution induced by human activities in Burullus Lake using Landsat 8 operational land imager and GIS. Egypt. J. Remote Sens. Space Sci., 20: S49-S56.

Gholizadeh, M.H., Melesse, A.M. and Reddi, L. 2016. A comprehensive review on water quality parameters estimation using remote sensing techniques. Sensors, 16(8): 1298.

Goetz, S., Gardiner, N. and Viers, J. 2008. Monitoring freshwater, estuarine and near-shore benthic ecosystems with multi-sensor remote sensing: An introduction to the special issue. Remote Sens. Environ., 112(11): 3993-3995.

Hadjimitsis, D.G., Hadjimitsis, M.G., Toulios, L. and Clayton, C. 2010. Use of space technology for assisting water quality assessment and monitoring of inland water bodies. Phys. Chem. Earth Parts A/B/C, 35(1-2): 115-120.

Hereher, M., Salem, M. and Darwish, D. 2010. Mapping water quality of Burullus Lagoon using remote sensing and geographic information system. J. Am. Sci., 7(1): 138-143.

Issa, I., Al-Ansari, N., Sherwany, G. and Knutsson, S. 2013. Trends and future challenges of water resources in the Tigris–Euphrates Rivers basin in Iraq. Hydrol. Earth Syst. Sci. Discussions, 10(12): 14617-14644.

Japitana, M.V. and Burce, M.E.C. 2019. A satellite-based remote sensing technique for surface water quality estimation. Eng. Technol. Appl. Sci, Res., 9(2): 3965-3970.

Kibena, J., Nhapi, I. and Gumindoga, W. 2014. Assessing the relationship between water quality parameters and changes in land use patterns in the Upper Manyame River, Zimbabwe. Phys. Chem. Earth, Parts A/B/C, 67: 153-163.

Kontopoulou, E., Kolokoussis, P. and Karantzalos, K. 2017. Water quality estimation in Greek lakes from Landsat 8 multispectral satellite data. Europ. Water, 58: 191-196.

Markogianni, V., Kalivas, D., Petropoulos, G.P. and Dimitriou, E. 2018. An appraisal of the potential of Landsat 8 in estimating chlorophyll-a, ammonium concentrations, and other water quality indicators. Remote Sens., 10(7): 1018.